AFCRL-72-0077

Distribution of Water Vapor in the Stratosphere as Determined from Balloon Measurements of Atmospheric Emission Spectra in the 24 - 29μm Region

by

Aharon Goldman, David G. Murcray, Frank H. Murcray
Walter J. Williams, James N. Brooks

Department of Physics
University of Denver
Denver, Colorado 80210

Contract No. F19628-71-C-0171
Project No. 8692

Scientific Report No. 1
February, 1972

Contract Monitor: Robert A. McClatchey
Optical Physics Laboratory

Sponsored by
Advanced Research Projects Agency
ARPA Order No. 1366
Monitored by
AIR FORCE CAMBRIDGE RESEARCH LABORATORIES
AIR FORCE SYSTEMS COMMAND
UNITED STATES AIR FORCE
BEDFORD, MASSACHUSETTS 01730

Program code no..... IE50

Effective date of contract.....26 March 1971

Contract expiration date.....29 February 1972

Principal investigator & phone no.....Dr. David G. Murcray/303 753-2627

Project Scientist & phone no.....Dr. Robert A. McClatchey/617 861-3224

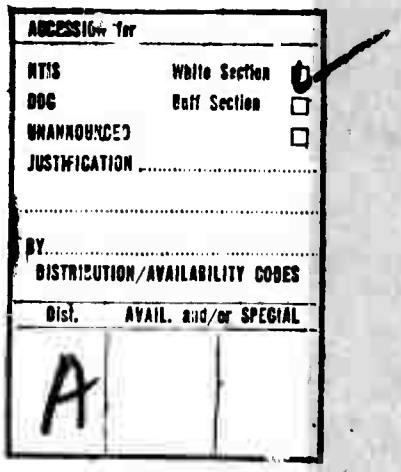

Qualified requestors may obtain additional copies from the Defense Documentation Center. All others should apply to the National Technical Information Service.

Unclassified

Security Classification

DOCUMENT CONTROL DATA - R & D

(Security classification of title, body of abstract and indexing annotation must be entered when the overall report is classified)

1. ORIGINATING ACTIVITY (Corporate author)
University of Denver
Department of Physics
Denver, Colorado 80210

2a. REPORT SECURITY CLASSIFICATION
Unclassified

2b. GROUP

3. REPORT TITLE
DISTRIBUTION OF WATER VAPOR IN THE STRATOSPHERE AS DETERMINED FROM BALLOON MEASUREMENTS OF ATMOSPHERIC EMISSION SPECTRA IN THE 24μm - 29μm REGION

4. DESCRIPTIVE NOTES (Type of report and inclusive dates)
Scientific Interim

5. AUTHOR(S) (First name, middle initial, last name)
Aharon Goldman
David G. Murcray
Frank H. Murcray
Walter J. Williams
James N. Brooks

6. REPORT DATE
February 1972

7a. TOTAL NO. OF PAGES
38

7b. NO. OF REFS
54

8a. CONTRACT OR GRANT NO.
F19628-71-C-0171 ARPA Order No. 1366

b. PROJECT NO.
Project, Task, Work Unit Nos.

c. 8692 n/a n/a

DoD Element 62301D

d. Dod Subelement n/a

9a. ORIGINATOR'S REPORT NUMBER(S)
Scientific Report No. 1

9b. OTHER REPORT NO(S) (Any other numbers that may be assigned this report)
AFCRL-72-0077

10. DISTRIBUTION STATEMENT

A - Approved for public release; distribution unlimited.

11. SUPPLEMENTARY NOTES
This research was supported by the Advance Research Projects Agency.

12. SPONSORING MILITARY ACTIVITY
Air Force Cambridge Research Laboratories (OP)
L. G. Hanscom Field
Bedford, Massachusetts 01730

13. ABSTRACT

The stratospheric water vapor mixing ratio altitude profile has been derived from spectral observations of the downward night emission from the pure rotation water vapor lines in the 24 - 29μm region of the spectrum. The data were obtained during two balloon flights, made on 22 February 1971 and on 29 June 1971, using a balloon-borne spectral radiometer with ~2 cm^{-1} resolution. The observed radiances have been fitted to line by line - layer by layer radiance calculations, from which the water vapor mixing ratio between 10 and 30 km has been derived. The resulting mixing ratio altitude profiles from both flights show a broad minimum around 15 km and a broad maximum around 25 km, with a range of values of 6×10^{-7} g/g to 4×10^{-6} g/g.

DD FORM 1 NOV 65 1473

Unclassified

Security Classification

14 KEY WORDS	LINK A		LINK B		LINK C	
	ROLE	WT	ROLE	WT	ROLE	WT
Infrared Emission Spectra						
Line by Line Model						
H_2O Mixing Ratio						

AFCRL-72-0077

Distribution of Water Vapor in the Stratosphere as Determined from Balloon Measurements of Atmospheric Emission Spectra in the 24 - 29μm Region

by

Aharon Goldman*, David G. Murcray, Frank H. Murcray
Walter J. Williams, James N. Brooks

Department of Physics
University of Denver
Denver, Colorado 80210

Contract No. F19628-71-C-0171
Project No. 8692

Scientific Report No. 1
February, 1972

*On leave from the Department of Environmental Sciences, Tel-Aviv University, Tel-Aviv, Israel

Contract Monitor: Robert A. McClatchey
Optical Physics Laboratory

Sponsored by
Advanced Research Projects Agency
ARPA Order No. 1366
Monitored by
AIR FORCE CAMBRIDGE RESEARCH LABORATORIES
AIR FORCE SYSTEMS COMMAND
UNITED STATES AIR FORCE
BEDFORD, MASSACHUSETTS 01730

ABSTRACT

The stratospheric water vapor mixing ratio altitude profile has been derived from spectral observations of the downward night emission from the pure rotation water vapor lines in the 24 - 29μm region of the spectrum. The data were obtained during two balloon flights, made on 22 February 1971 and on 29 June 1971, using a balloon-borne spectral radiometer with ~2 cm^{-1} resolution. The observed radiances have been fitted to line by line - layer by layer radiance calculations, from which the water vapor mixing ratio between 10 and 30 km has been derived. The resulting mixing ratio altitude profiles from both flights show a broad minimum around 15 km and a broad maximum around 25 km with a range of values of 6×10^{-7} g/g to 4×10^{-6} g/g.

Table of Contents

LIST OF FIGURES

LIST OF TABLES

I. INTRODUCTION

A number of spectroscopic derivations of the water vapor vertical distribution in the atmosphere have been made. The earlier spectroscopic measurements were made from observations of the absorption of the solar infrared spectrum from aircraft[1-5] and balloons.[6-19] More recently, water vapor amounts have been inferred from infrared radiometric measurements of the water vapor emission spectrum. These include data from balloon-borne radiometers used to observe the infrared downward and upward emission[20-24] and satellite-borne radiometers used to observe the upward emission[25-31] and the limb emission.[32, 33]

H_2O mixing ratios derived from these data show considerable divergence, especially for the middle stratosphere. The results for the lower stratosphere are less contradictory and most of the spectroscopic derivations yield a "dry" lower stratosphere, with mixing ratios close to 2×10^{-6} g/g. Almost all of the frost point measurements support these results.[34-37] However, despite the numerous experiments, the distribution of water vapor in the middle stratosphere is rather uncertain. Some results indicate that the mixing ratio remains close to the "dry" value of the lower stratosphere, while others indicate that the mixing ratio increases again at the middle stratosphere. Comparison of the different results leads to uncertainties of one to two orders of magnitude.

It is evident that more accurate determinations of H_2O concentrations in the middle stratosphere are needed. This is difficult to obtain with the absorption spectra method. The basic limitation of this method is that such data, even with high resolution of ~ 0.25 cm^{-1} as obtained during recent balloon flights,[38, 39] cannot be used to meaningfully measure spectrally degraded emissivities which are smaller than a few per cent. On the other hand, a sensitive cooled spectral radiometer can measure spectrally degraded emissivities of $<10^{-3}$. Thus, if the spectral radiometer

can resolve line groups, the spectral emission method offers significant advantages for the determination of small gas amounts in the upper atmosphere.

In the present study, the infrared spectral emission method is applied to the derivation of the H_2O distribution in the stratosphere using the spectral radiance data obtained during two recent balloon flights, made on February 22, 1971, and June 29, 1971, from Holloman Air Force Base, New Mexico. During these flights, spectral observations of atmospheric downward night emission were obtained in the 16 - 30μm region of the spectrum. Spectral scans were made from a number of altitudes up to 30 km, with a balloon-borne grating radiometer system. The grating spectrometer was cooled with liquid nitrogen to reduce the thermal background, thus increasing the sensitivity of the liquid helium cooled Cu:Ge detector. The resolution obtained is better than 2 cm^{-1} near 25μm.

The 16 - 30μm region of the atmospheric emission spectrum contains line features due to CO_2, N_2O, HNO_3 and H_2O, as has been verified from the high resolution solar absorption spectra observed in this region with a balloon-borne spectrometer.[39] In the long wavelength interval of this region, between 24μm, and 30μm, the effect of CO_2, N_2O and HNO_3 is negligible, and the observed emission is mainly due to pure rotation H_2O lines.

The individual H_2O line parameters (positions, intensities, half-widths and energy levels) are known for this spectral region, hence it is possible to derive the atmospheric vertical distribution of H_2O on a line by line basis. The measurements were obtained from many altitudes, so that the atmosphere can be divided into a number of layers and the line by line technique can be applied to a layer by layer inferrence of the H_2O profile. Such a method of analysis is described in Section II. The resulting profiles from the two balloon flights are described in Section III, followed by a discussion of the technique in Section IV and the conclusions in Section V.

II. METHOD OF ANALYSIS

The radiometric measurements are made from different altitudes $h_1, h_2, \ldots, h_N$ at a constant zenith angle of 45^o. The atmosphere is assumed to be stratified into layers defined by actual altitudes of observation. The analysis starts at the highest altitude of observation h_1, at the smallest radiance values, and then proceeds layer by layer, to the lower altitudes with increasing radiance values. The residual atmosphere above h_1 is considered as one homogenous layer, so that the infinite resolution radiance at wavenumber $\nu(cm^{-1})$ to be observed at altitude h_1, $R(\nu, h_1)$, is a one layer emission according to[40]

$$R(\nu, h_1) = \epsilon(\nu, 1)\, B(\nu, 1), \tag{1}$$

where $B(\nu, 1)$ is the black body radiance at temperature θ_1 of layer 1, and $\epsilon(\nu, 1)$ is the infinite resolution emissivity of this layer. The atmosphere below h_1 is divided into N-1 homogenous layers, defined by $h_2, h_3, \ldots, h_N$. The emission from the first layer is transmitted through the second layer according to $\tau(\nu, 2)\, R(\nu, h_1)$, where $\tau(\nu, 2)$ is the infinite resolution transmittance of the second layer. In addition, the second layer emits radiance according to $\epsilon(\nu, 2)\, B(\nu, 2)$. Thus, the infinite resolution radiance observed at h_2, $R(\nu, h_2)$, is given by

$$R(\nu, h_2) = \tau(\nu, 2)\, R(\nu, h_1) + \epsilon(\nu, 2)\, B(\nu, 2). \tag{2}$$

This process proceeds through all the layers below h_1 according to

$$R(\nu, h_n) = \tau(\nu, n)\, R(\nu, h_{n-1}) + \epsilon(\nu, n)\, B(\nu, n), \tag{3}$$

for $n = 2, \ldots, N$.

Eqs. (1) - (3) represent successive equations for $R(\nu, h_n)$, where each step below h_1 involves two consecutive layers. (See Appendix)

Assuming no scattering, the relation $\tau(\nu) = 1 - \epsilon(\nu)$ will hold for thermodynamical equilibrium and this can be substituted into Eqs. (1) - (3). $\tau(\nu, h_n)$ is a function of the amount of water vapor U(n) in the layer n between

altitudes h_n and h_{n-1}. It seems now that once a theoretical model is developed for $\tau(\nu, h_n)$, Eqs. (1) - (3) can be solved successively for U(n), n = 1,...,N, thus yielding the desired H_2O profile. However, the observed spectral radiance, $\bar{R}(\nu, h_n)$, is not at infinite resolution, but is rather a convolution of the infinite resolution radiance $R(\nu, h_n)$, with the spectrometer slit function $g(\nu-\nu')$ according to[40]

$$\bar{R}(\nu, h_n) = \int_{\nu-a}^{\nu+a} R(\nu, h_n)\, g(\nu-\nu')d\nu' / \int_{\nu-a}^{\nu+a} g(\nu-\nu')d\nu', \tag{4}$$

where $2a(cm^{-1})$ is the spectral width of the slit function.

The integrated radiance though, is independent of the slit function[40] so that:

$$\int_{\nu_1}^{\nu_2} R(\nu, h_n)d\nu = \int_{\nu_1}^{\nu_2} \bar{R}(\nu, h_n)d\nu, \tag{5}$$

where ν_1 and ν_2 are the limits of the spectral region under consideration. Thus, the integrated radiance is a suitable parameter for a fitting of theoretical integrated radiance, $\int R(\nu, h_n)d\nu$, to the experimental values, $\int \bar{R}(\nu, h_n)d\nu$, by successive solutions of the equations:

$$F[U(n)] \equiv \int_{\nu_1}^{\nu_2} R(\nu, h_n)d\nu - \int_{\nu_1}^{\nu_2} \bar{R}(\nu, h_n)d\nu = 0, \tag{6}$$

for U(n), n = 1,...,N, where $R(\nu, h_n)$ is given by Eqs. (1) - (3).

It is not necessary here to use the entire band, but only to pick out an interval $[\nu_1, \nu_2]$ with a representative isolated group of lines. It is important that the spectral region chosen will be isolated, so that the experimental integrated radiance can be accurately determined.

The above determination of U(n) requires a suitable model for the calculation of $\tau(\nu, n)$. The most accurate transmittance is obtained by a line by line calculation. The monochromatic transmittance $\tau(\nu, n)$ is given by[41]

$$\tau(\nu, n) = \exp[-k(\nu, n)\, U(n)], \tag{7}$$

where $k(\nu, n)$ is the absorption coefficient, which is a sum of the absorption coefficients of all spectral lines,

$$k(\nu, n) = \sum_i k_i(\nu, n), \tag{8}$$

which might contribute to the transmittance at ν.

The atmospheric infrared line shapes are given by the Voigt profile,[40,41] which is a convolution of the Lorentz and Doppler shapes. The Doppler halfwidth, α_D, is given by

$$\alpha_D\,(\mathrm{cm}^{-1}) = 3.58 \times 10^{-7}\ \nu_0\,(\mathrm{cm}^{-1})\,[\theta(\mathrm{K})/M]^{1/2}, \tag{9}$$

where ν_0 is the line position, T the temperature and M the molecular weight. At θ = 225K, ν = 350 cm^{-1}, the Doppler half width is α_D = 0.0004 cm^{-1}. Typical collision halfwidths are $\alpha_L \sim 0.08\ \mathrm{cm}^{-1}\ \mathrm{atm}^{-1}$. Thus, $\alpha_D \sim \alpha_L$ only at about 5 mb (~36 km) and Doppler effects can be neglected at the altitudes of interest (10 - 30 km). Thus,

$$k(\nu, n) = \sum_i \frac{S^o{}_i(n)}{\pi} \quad \frac{\alpha_i(n)}{(\nu - \nu_{oi})^2 + \alpha^2{}_i(n)}, \tag{10}$$

where ν_{oi}, α_i, and $S^o{}_i$ are the individual line centers, line halfwidths and line intensities respectively. The individual H_2O line parameters for the region of interest have been compiled under the AFCRL Atmospheric Transmittance Program.[42] In the atmosphere, α_i and $S^o{}_i$ will vary from one layer to another as a result of temperature and pressure variations. The line intensities are assumed to depend on the temperature θ according to[40]

$$S^o(\theta) = S^o(\theta_o)\,[\theta_o/\theta]^{3/2}\ \exp[-1.439E''(1/\theta - 1/\theta_o)][1-\exp(-1.439\nu_o/\theta)]$$

$$/[1-\exp(-1.439\nu_o/\theta_o)], \tag{11}$$

where E'' (cm^{-1}) is the lower state energy, θ_o, θ are in Kelvins, and ν_o (cm^{-1}) is the line position. The induced emission term, normally neglected in the near infrared region, is included here, since it becomes significant at these longer wavelengths. At θ = 225K and θ = 300K, $1-\exp(-1.439\,\nu_o/\theta) \sim 0.96$ and ~ 0.91 respectively even for ν_o = 500 cm^{-1}.

The pressure dependence of α in an homogenous layer is $\alpha = \alpha^o P_e$ where P_e is the effective pressure for H_2O - N_2 mixture, given by [43-45]

$$P_e = P_t + 4p, \tag{12}$$

where P_t is the total pressure of the gas mixture and p is the partial pressure of the absorbing gas. For atmospheric H_2O, p is small so that $P_e \sim P_t$. The temperature dependence of α is assumed to be[46]

$$\alpha^o(\theta) = \alpha^o(\theta_o)\,(\theta_o/\theta)^{0.62}. \tag{13}$$

Atmospheric temperature and pressure profiles can be obtained from sondes data taken during the radiance measurements. The Curtis-Godson approximation[41] is then used to derive average temperatures $\overline{\theta}_n$ and pressure $\overline{P}_n$ for each homogenous layer. A constant H_2O mixing ratio is assumed within each layer, so that[41]

$$\overline{P_n} = 0.5\,(P_n + P_{n-1}), \tag{14}$$

where P_n is the atmospheric pressure measured at altitude h_n. A similar relation is assumed for the temperature $\overline{\theta}_n$. These expressions for average pressures and temperatures are used for $n \geq 2$ while for n = 1 $\overline{P}_1$ is taken as $P_1/2$ and $\overline{\theta}_1$ as θ_1.

With the assumptions made above for the transmittance calculation one can proceed to the solution of Eq. (6). It turns out that the Newton-Raphson iterative method[47] is very efficient for the solution for U(n). The iterations are made according to

$$U^{i+1}(n) = U^i(n) - F[U(n)] \,/\, F'[U(n)], \tag{15}$$

where the prime denotes the derivative with respect to U(n), and $U^i(n)$ is an approximation for the zero of F[U(n)]. The derivative is given by

$$F'[U(n)] = \int_{\nu_1}^{\nu_2} -k(\nu, n) \exp[-k(\nu, n)\ U(n)]\ R(\nu, h_{n-1})d\nu$$

$$+ \int_{\nu_1}^{\nu_2} k(\nu, n) \exp[-k(\nu, n)\ U(n)]\ B(\nu, n)d\nu, \qquad (16)$$

for $n > 1$, while for $n = 1$ the first term is omitted. The absorption coefficients $k(\nu, n)$ have to be computed only once for each layer, and are not changed during the iterations.

A computer program has been developed to derive the H_2O profile according to the method outlined above. The computation of $k(\nu, n)$ has been made by subroutines previously developed by T. G. Kyle.[48] The program can also produce a degraded emission spectra for a given H_2O profile. Thus, once values for U(n) are derived, the calculated degraded spectra can be compared with the measured degraded spectra, for any altitude h_n.

Despite the apparent simplicity of the equations involved, large high speed computers are needed to make such computations practical. A 10 layer calculation for a 15 cm^{-1} interval with 4 iterations per layer takes ~60 seconds on the CDC 7600 at NCAR, Boulder. This is mainly due to the fine net needed for the calculation of the absorption coefficients and due to the fact that each step in the layer by layer calculation involves the radiances from two layers (except for the first layer). A fine net interval of 0.001 cm^{-1} was needed for the upper layers due to the small atmospheric pressures.[49]

F[U(n)] is a smooth function of U(n), so that with a reasonable guess for an initial approximation, the single zero of F can be found to 4 - 5 significant figures withing 3 to 5 iterations. However, an improper value for the initial approximation $U^1(n)$ may yield a negative value for $U^2(n)$ so that a new $U^1(n)$ has to be tried. The same iteration procedure is

repeated for each new layer, until the complete H_2O profile is derived.

III. RESULTS

Selected records of the emission spectra obtained in the 16 to 30μm region during the balloon flight made 22 February 1971 are shown in Fig. 1. The radiance scale for each record is from 10^{-7} to 10^{-4} w cm^{-2} $sr^{-1}\mu^{-1}$ and each record is offset from the next by two decades. The zenith angle was 45° for all records. The times, altitudes, pressures and temperatures are shown in Table I. The results of the 29 June 1971 flight show similar spectral patterns, but with somewhat different values of radiances as a function of altitude. Temperature and pressure data for the two flights were obtained from rawinsonde ascents made at the same time and place as the primary flights. The rawinsonde data obtained during the February flight are not complete, so that it was necessary to supplement the data on the basis of rawinsonde data obtained at Holloman on different dates, and on the basis of the U. S. Standard Atmosphere.[50] Complete rawinsonde pressure and temperature data were obtained during the June flight and these values were used for the data analysis.

Examination of Fig. 1 shows that for wavelengths larger than 24μm the radiance is dominated by H_2O pure rotation lines, degraded to several line groups by the spectrometer slit function. The line group near 25μm is particularly well isolated, and can be used to fit $\int R(\lambda, h_n)d\lambda$ to $\int \overline{R}(\lambda, h_n)d\lambda$ as described in Section II. The spectral region of this group extends from 389 to 405 cm^{-1}, and contains 9 strong H_2O lines and 18 much weaker lines.[42] Each one of the strong lines is overlapped to some extent by one or more of the other strong lines, and the measured radiance shows how these are degraded to 3 distinct peaks. The measured integrated radiance values of the 25μm line group are given in the last column of Table I.

Starting with one layer above float altitude, U(1) has been derived from the 25μm line group, yielding a mixing ratio of 5.8×10^{-6} g/g for the February flight. This value of U(1) has been used to compute a degraded spectrum for the 20 - 30μm region, shown in Fig. 2. It is seen

that while near 20μm the resolution of the calculated spectrum is higher than that of the experimental spectrum, the opposite is the case near 30μm. This is due to the fact that a constant wavenumber slit function (in this case a Gaussian function with a halfwidth of 0.90 cm^{-1}) has been used for the calculated spectrum, while the experimental grating spectra has roughly a constant wavelength resolution. The integrated radiances are not effected by the slit function and it is seen that even though U(1) was derived from the 25μm line group only, the agreement between the calculated and experimental radiance is very good through out the whole region.

Similar comparisons for several layer calculations over short intervals within the 24 - 29μm region show the same agreement. In particular, 10 layer calculations for both the 25μm line group and the 26μm line group, yield very close profiles. Thus, it was concluded that only the 25μm line group will be used for the derivation of the water vapor profile. This reduces considerably the computer time and allows the use of 15 atmospheric layers in the computation without exceeding 1 minute of computing time of the CDC 7600.

The results for U(n) from a 15 layer calculation, where the layers are defined by the records in Fig. 1 for the February flight are shown in Fig. 3. The histogram representation shows the thickness of the layers and stresses the fact that a constant mixing ratio is assumed within each layer. The calculated and experimental radiance at the lowest altitude, h_{15} = 8.6 km, are shown in Fig. 4. Results from a 15 layer calculation for the June flight are also shown in Fig. 3.

The number of layers was limited to 15 even though more records were obtained at intermediate altitudes. The resulting altitude resolution shown in Fig. 3 is about 2 km near float altitude, gradually increasing to ~0.5 km near 10 km. This variable altitude resolution has been chosen on the basis of the diminishing rate of the radiance decrease with altitude, as evident in Fig. 1 and Table I. The altitude resolution will increase by increasing the spectral interval. A test for the validity of the February pro-

file shown in Fig. 3 was made by deriving a 10 layer profile in which some of the layers from the 15 layer calculation were doubled in thickness. The results are shown by a broken line on Fig. 3, and it can be seen that these actually represent some average of the 15 layer profile.

Some data are missing between 11 and 18 km on the June flight so that some of the altitude interval sizes are not optimum whithin this altitude range.

Fig. 3 shows that for February, 1971, the water vapor mixing ratio above 29.3 km is about 6×10^{-6} g/g and for June, 1971, about 4×10^{-6} g/g. The present method does not infer the distribution above float altitude so that these values represent the total amount of water vapor above float if the water vapor were uniformly mixed. Both the February and June profiles show a broad minimum extending from 12 to 18 km, with a mixing ratio of $\lesssim 1 \times 10^{-6}$ g/g. The mixing ratio increases above this altitude, forming a broad maximum near 24 or 25 km. The mixing ratio may decrease again above 25 km, but must increase at some higher altitude to account for the observed radiance values at float altitude. The minimum near 15 km and the maximum near 25 km are distinct features of both flights, even though the minimum and the maximum are lower on the June flight.

IV. DISCUSSION

The above analysis of the spectral radiance data should be examined in detail to determine the possible sources of error and their magnitude. Both the theoretical parameters and the experimental data may contribute errors. The theoretical parameters are discussed in detail in this section and wherever possible, the experimental parameters are also considered.

The present formulation uses an isotropic steady state model, which does not take into account the time and position variations of H_2O radiance values from different layers. Once a U(n) is derived, the same U(n) is used to derive U(n+1), even though the measurements at h_n at h_{n+1} are not simultaneous in time and location; they are made during ascent or descent of the balloon, which will drift a number of miles during a flight.

The present model applies to spectral regions which are dominated by lines centers and not by wings. Emissions from clouds or particle layers are not taken into account, thus assuming a "clear" atmosphere. This avoids the uncertainty in the absorption coefficient of the continuum and the unsatisfactory representation of the line wings by the Lorentz profile.

Within these limitations, the iteration procedure can fit U(n) to satisfy Eq. (6) to any arbitrary accuracy; but the significant digits in U(n) are limited by the accuracy of the experimental values $\overline{R}(\nu, h_n)$, of the individual line parameters and of the atmospheric temperatures and pressures. Line positions are known to high precision (6 to 7 significant figures) but line intensities and line halfwidth are not known to better than 10 to 20%. This obviously limits the accuracy of the transmittance determination. The uncertainties in atmospheric temperature and pressure data effect both the transmittance and the radiance values. Trial runs with a number of atmospheric temperature profiles showed that errors of 3 - 4K will not effect the derived U(n) by more than 5%. The error in U(n) due to errors in S^o and α can then be inferred from the square root approximation for a single line, $[S^o \alpha\, U(n)]^{1/2}$. Trial runs for a few layers with dif-

ferent values for S^{o} and α have verified this estimate of error. Since 10% error is typical for S^{o} and α, the square root relation may increase the associated error in U(n) to 40%.

There are two effects these errors can have on the water vapor mixing ratio. They can influence the absolute accuracy of the derived values of U(n) and of the relative values of U(n) at different altitudes. The absolute values have a greater uncertainty than the relative values. This is important to stress because the uniqueness of the present altitude mixing ratio profiles is in their relative values between 10 and 30 km. The resultant absolute error, based on the above estimates of 10% for S^{o} and α 5% for atmospheric temperature and allowing 10 to 15% error in the experimental measurement of $\overline{R}$, is up to 60% of the absolute values of U(n). The relative values seem to be accurate within 5 to 10%.

In evaluating possible errors, one additional consideration must be made. Previous studies have shown that stratospheric water vapor measurements may be subject to errors due to local moisture contamination. Most of these studies involve measurements of the water vapor content in the immediate vicinity of the instrument package. The contamination must occur over a significant path length before it is important in an infrared emission study. This path can be considered in two parts, that which is internal to the instrument and that which is external to it, but still influenced by the balloon train dynamics.

Laboratory studies have established that there is no measurable water vapor contamination within the spectral radiometer. This is due to the low operating temperature of the radiometer combined with the nitrogen venting system. The external optical path is relatively short compared with the path from the atmospheric layers being considered and would require considerable contamination to influence the results significantly. There is good evidence to indicate that this amount of contamination is not present. Water vapor emission data associated with the flights analyzed here show that when measurements made during ascent were compared

with those made during descent, the values were identical at similar altitudes. Such measurements preclude the possibility of any significant amount of water being swept down from the balloon vehicle. In addition, similar data collected over an hour or more at float altitude showed no significant increase or decrease in the amount of vapor in the emitting path.

V. CONCLUSIONS

On the basis of these results, some of the fine structure in the inferred H_2O profiles might be artificial, but the gross vertical structure with the broad maximum near 25 km seems to be real. The maximum indicates a relatively "wet" atmospheric layer near 25 km. The origin of such a layer is not obvious and might be related to the photochemical processes in the O_3, HNO_3, NO_2 layer. Comparison of the profiles from the 22 February 1971 and 29 June 1971 flights indicate that a seasonal variation might exist. During summer, both the minimum near 15 km and the maximum near 25 km are smaller than that during the winter. Additional measurements are obviously required to establish seasonal variations in the water vapor profile.

The procedure developed in the present study can be applied to other types of layer by layer radiance calculations. The inference of H_2O profiles from upward emission measurements from balloons or satellites can be accomplished with the same procedure used here, only reversed in the order of altitudes, and the earth emission term has to be included. Limb radiance scans from satellites can be treated in a similar manner even though the geometry of the experiment is different. The technique is not limiited to H_2O only, and can be applied to other minor atmospheric constituents. The basic requirements for such an application are that spectral line features can be isolated, either by a spectrometer or by a narrow filter, that the corresponding individual line parameters will be known, and that the geometry of the experiment will define atmospheric layers by the actual altitudes or angles of observations. Line by line - layer by layer radiance analysis is then an efficient method for deriving the vertical distribution of minor atmospheric constituents.

VI. APPENDIX

It can be shown that the formulation given by Eqs. (1) - (3) are mathematically equivalent to the more commonly used expression

$$R(\nu, h_n) = \sum_{m=n}^{l} B(\nu, m)\,[T(\nu, n, m+1) - T(\nu, n, m)], \qquad \text{(A-1)}$$

where

$$T(\nu, n, m) = \prod_{j=n}^{m} \tau(\nu, j), \qquad \text{(A-2)}$$

and

$$T(\nu, n, n+1) = 1.$$

$T(\nu, n, m)$ is the combined transmittance through layer n to m. Eq. (A-1) is the representation in terms of layers of the integral form of the radiative transfer equation[41] with a zero boundary term:

$$R(\nu, h_n) = \int_{h_n}^{\infty} B(\nu, h) \frac{\partial T(\nu, h)}{\partial h} dh, \qquad \text{(A-3)}$$

where $T(\nu, h)$ is the spectral transmittance at height h.

Eq. (3) is more convenient than Eq. (A-1) for layer by layer derivations of U(n), while Eq. (A-1) is more convenient when one layer is assumed from each altitude h_n to the top of the atmosphere. However, in both representations, improper evaluation of the transmittance terms might lead to serious errors in U(n). The basic difficulty is that the expressions for $R(\nu, h_n)$ in Eqs. (3) and (A-1) are valid for infinite resolution only. The infinite resolution transmittance values for the stronger of the H_2O lines in the 20 - 30μm region over atmospheric paths of $\gtrsim$ 1 km approach the square root region of the curve of growth even near 30 km altitude. This prohibits the use of a number of simplifications that could have been made. For example, the approximation

$$\int R(\nu, h_{n-1})\, \tau(\nu, n)d\nu \sim \int R(\nu, h_{n-1})d\nu, \qquad \text{(A-4)}$$

might have simplified the analysis to

$$\Delta R = \int R(\nu, h_n)d\nu - \int R(\nu, h_{n-1})d\nu = \int [1-\tau(\nu, n)]\, B(\nu, n)d\nu \qquad \text{(A-5)}$$

where ΔR represents the difference in integrated radiance observed at two consecutive altitudes. Eq. (A-5) reduces the problem to a one layer calculation for each layer, but the approximation in Eq. (A-4) is not valid unless $\tau(\nu, n)$ is in the linear region of the curve of growth. In order to demonstrate the possible error associated with this approximation, trial runs were made with two layers, the first from 29.3 km to the top of the atmosphere and the second between 25.2 km and 29.3 km. The results show that U(2) as derived from Eq. (A-5) is about 4 times smaller than U(2) as derived from Eq. (6).

It should be noted that the square root region implies a strong pressure dependence of the emission. As a result, the inferred mixing ratio for large enough layers will be biased by the higher pressure levels. Trial runs with $\gtrsim$10 km layers between 12.5 to 25 km verify that and yield mixing ratio values which are close to the minimum values obtained from the 10 and 15 layer calculations.

Another difficulty is that the infinite resolution $\tau(\nu, n)$ cannot arbitrarily be replaced by some average transmittance values $\bar{\tau}(\nu, n)$, as derived from a band model theory or from degraded spectra. This is due to the fact that $R(\nu, h_n)$ involves products of the type $T(\nu, n, m)$ given in Eq. (A-2), and for such products

$$\int \prod_i \tau(\nu, i)d\nu \neq \int \prod_i \bar{\tau}(\nu, i)d\nu, \qquad \text{(A-6)}$$

unless all $\tau(\nu, i)$ are in the linear region. The error involved in Eq. (A-6) for a two layer calculation has been studied,[50-54] and it has been shown that an overlap correction is needed, the neglecting of which can lead to

large errors in the inferred gas amounts.

It follows from the previous discussion that proper evaluation of the transmittance is critical for the calculations of integrated radiance for a layered atmosphere. In the present analysis, the difficulties have been eliminated by performing exact line by line transmittance computations.

VII. ACKNOWLEDGEMENTS

The research was supported in part by the Advanced Research Projects Agency and was monitored by the Air Force Cambridge Research Laboratories. The launch and recovery of the balloon instrumentation was capably handled by the Air Force Cambridge Research Laboratories Balloon Group.

Acknowledgement is made to the National Center for Atmospheric Research, which is sponsored by the National Science Foundation, for computer time used in this research. The authors are indebted to T. G. Kyle of the National Center for Atmospheric Research, Boulder, Colorado, for a copy of his program for evaluating the line by line transmittance. The computer programs for data reduction and plotting have been developed by J. Van Allen.

VIII. REFERENCES

1. J. T. Houghton and J. S. Seeley, Quart. J. Roy. Met. Soc. 86, 358 (1960).

2. F. Stauffer and J. Strong, Appl. Opt. 1, 129 (1962).

3. J. T. Houghton, Quart. J. Roy. Met. Soc. 89, 332 (1963).

4. C. Cumming, G. R. Hawkins, D. J. G. McKinnon J. Rollins and W. R. Stephenson, "Quantitative Atlas of Infrared Stratospheric Transmission in the 2.7 Micron Region", Canadian Armament Research and Development Establishment, CARDE Techn. Rept. 546/65 Project D46-38-01-19, (1965).

5. R. F. Calfee and D. M. Gates, Appl. Opt. 5, 287 (1966).

6. D. G. Murcray, F. H. Murcray, W. J. Williams, and F. E. Leslie, J. Geophys. Res. 65, 3641 (1960).

7. D. G. Murcray, J. N. Brooks, F. H. Murcray and W. J. Williams, J. Opt. Soc. Am. 50, 107 (1960).

8. D. G. Murcray, F. H. Murcray, W. J. Williams and F. E. Leslie, J. Opt. Soc. Am. 51, 186 (1961).

9. D. G. Murcray, F. H. Murcray and W. J. Williams, J. Geophys. Res. 67, 759 (1962).

10. D. G. Murcray, F. H. Murcray and W. J. Williams, J. Opt. Soc. Am. 54, 23 (1964).

11. D. G. Murcray, F. H. Murcray and W. J. Williams, J. Opt. Soc. Am. 55, 1239 (1965).

12. D. G. Murcray, F. H. Murcray and W. J. Williams, Quart. J. Roy. Met. Soc. 92, 159 (1966).

13. D. G. Murcray, T. G. Kyle and W. J. Williams, J. Geophys. Res. 74, 5369 (1969).

14. M. S. Kiseleva, B. S. Neporent and V. A. Fursenkov, Optics and Spectroscopy 6, 522 (1959).

15. M. S. Kiseleva and B. S. Neporent, Optics and Spectroscopy, 19 513 (1965).

16. B. S. Neporent, M. S. Kiseleva, A. G. Makogonenko and V. I. Schlyakhov, Appl. Opt. 6, 1845 (1967).

17. R. Zander, J. Geophys. Res. 71, 3775 (1966).

18. K. Ya Kondratiev, G. A. Nicolsky, I. Ya Badinov and S. D. Andreev, Appl. Opt. 6, 197 (1967).

19. D. H. Höhn Infrared Phys. 4, 239 (1964).

20. E. J. Williamson and J. T. Houghton, Quart. J. Roy. Met. Soc. 91, 330 (1965).

21. D. R. Pick and J. T. Houghton, Quart. J. Roy. Met. Soc. 95, 535 (1969).

22. B. J. Conrath, J. Geophys. Res. 74, 3347 (1969).

23. P. M. Kuhn and J. D. McFadden, Mon. Wea. Rev. 95, 565 (1967).

24. P. M. Kuhn and S. K. Cox, J. Appl. Meteor. 6, 142 (1967).

25. W. L. Smith, Mon. Wea. Rev. 95, 363 (1967).

26. W. L. Smith, Mon. Wea. Rev. 96, 387 (1958).

27. W. L. Smith, Appl. Opt. 9, 1193 (1970).

28. W. L. Smith and H. B. Howell, J. Appl. Meteor. 10, 1062 (1971).

29. F. Möller and E. Raschke, "Evaluation of Tiros 3 Radiation Data", Contractor Report CR-12, NASA, Washington, D. C., 1964.

30. E. Raschke and W. R. Bandeen, J. Appl. Meteor. 6, 468 (1967).

31. B. J. Conrath, R. A. Hanel, V. G. Kunde and C. Prabhakara, J. Geophys. Res. 75, 5831 (1970).

32. F. B. House and G. Ohring, "Inferrence of Stratospheric Temperature and Moisture Profiles from Observations of the Infrared Horizon", GCA Corp., NASA-CR-1419 (GCA-TR-59-5-N) Contract NAS 1-7572 (1969).

33. T. B. McKee, R. I. Whitman and J. J. Lambiotte Jr., "A Technique to Infer Atmospheric Water Vapor Mixing Ratio from Measured Horizon Radiance Profiles", Langley Res. Center, NASA TN D-5252 (1969).

34. M. Gutnick, J. Geophys. Res. 66, 2867 (1961).

35. J. H. Mastenbrook, J. Atm. Sci. 25, 299 (1968).

36. J. H. Mastenbrook, J. Atm. Sci. 28, 1495 (1971).

37. N. Sissenwine, D. D. Grantham and H. A. Salmela, J. Atm. Sci. 25, 1129 (1968).

38. D. G. Murcray, F. H. Murcray, W. J. Williams, T. G. Kyle and A. Goldman, Appl. Opt. 8, 2519 (1969).

39. D. G. Murcray, J. N. Brooks, J. J. Kosters and W. J. Williams, "Atmospheric Emission at High Altitudes", Department of Physics, Denver University, Denver, Colorado, Final Report AFCRL - 71 - 0359 (1971).

40. S. S. Penner, Quantitative Molecular Spectroscopy and Gas Emissivities, (Addison-Wesley, Reeding, Mass., 1959).

41. R. M. Goody, Atmospheric Radiation, Vol. I Theoretical Basis (Oxford University Press, New York, 1964).

42. High Resolution Atmospheric Transmittance Program, directed by R. A. McClatchey, Optical Physics Laboratory, Air Force Cambridge Research Laboratories, Bedford, Mass. 01730. The water vapor line parameters have been derived by W. S. Benedict.

43. D. E. Burch, E. B. Singleton and D. Williams, Appl. Opt. 1, 359 (1962).

44. D. E. Burch, W. L. France and D. Williams, Appl. Opt. 2, 585 (1963).

45. C. H. Palmer, J. Opt. Soc. Am. 50, 1232 (1960).

46. W. S. Benedict and L. D. Kaplan, J. Chem. Phys. 30, 388 (1959).

47. D. R. Hartree, Numerical Analysis, p. 214, (Oxford University Press, 1958).

48. T. G. Kyle, J. Quart. Spectr. Rad. Tran. 9, 1477 (1969).

49. T. G. Kyle, J. Opt. Soc. Am. 58, 192 (1968).

50. U. S. Standard Atmosphere, 1962. NASA, U. S. Air Force and U. S. Weather Bureau, Dec., 1962.

51. H. Sakai and F. R. Stauffer, J. Opt. Soc. Am. 54, 759 (1964).

52. G. D. Maclay and H. J. Babrov, J. Opt. Soc. Am. 54, 301 (1964).

53. G. N. Plass, Appl. Opt. 4, 161 (1965).

54. G. N. Plass, J. Opt. Soc. Am. 55, 104 (1965).

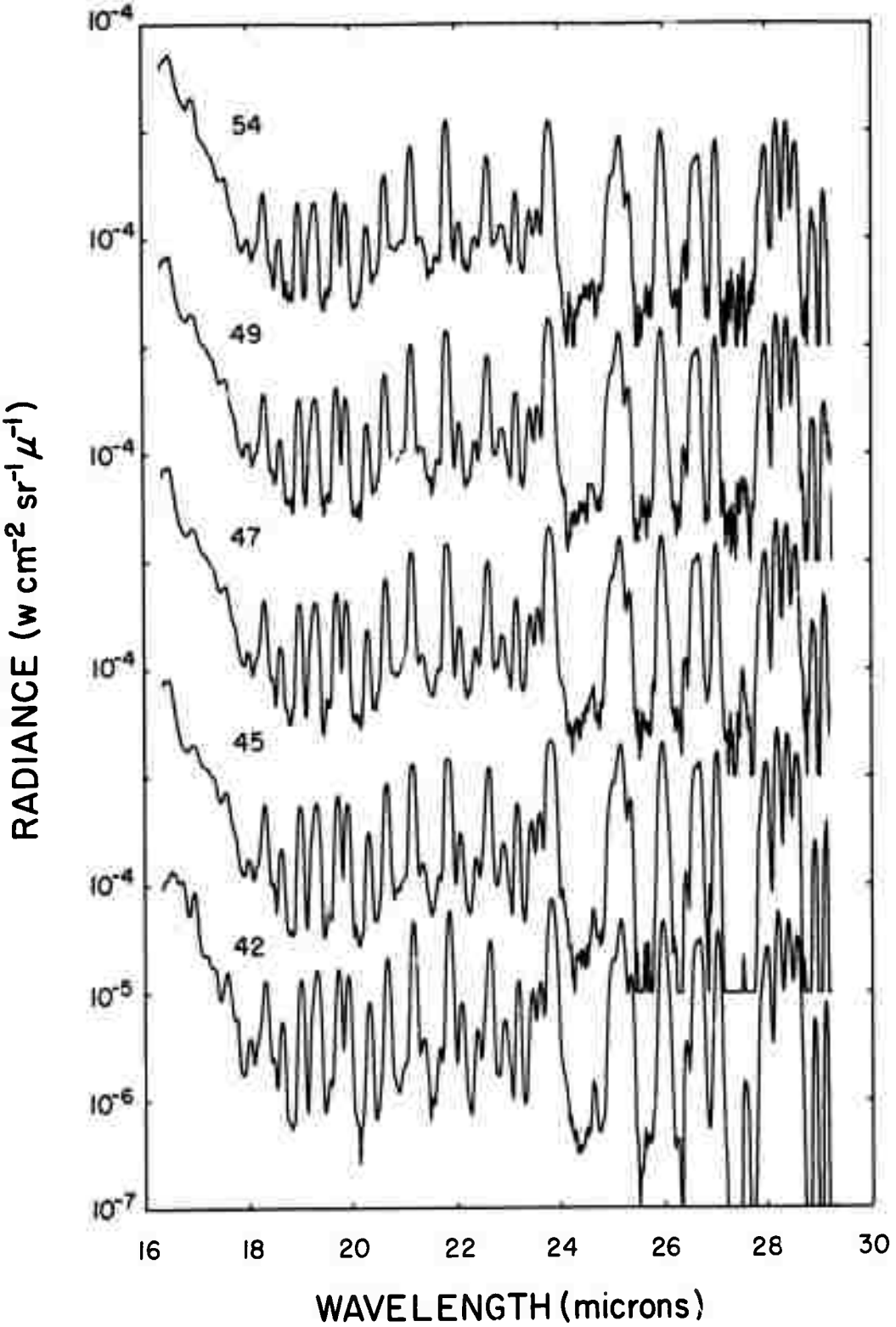
RADIANCE (w cm^{-2} sr^{-1} μ^{-1})
10^{-4}
10^{-4}
10^{-4}
10^{-4}
10^{-4}
10^{-5}
10^{-6}
10^{-7}
54
49
47
45
42
16
18
20
22
24
26
28
30
WAVELENGTH (microns)

Fig. 1 (a)

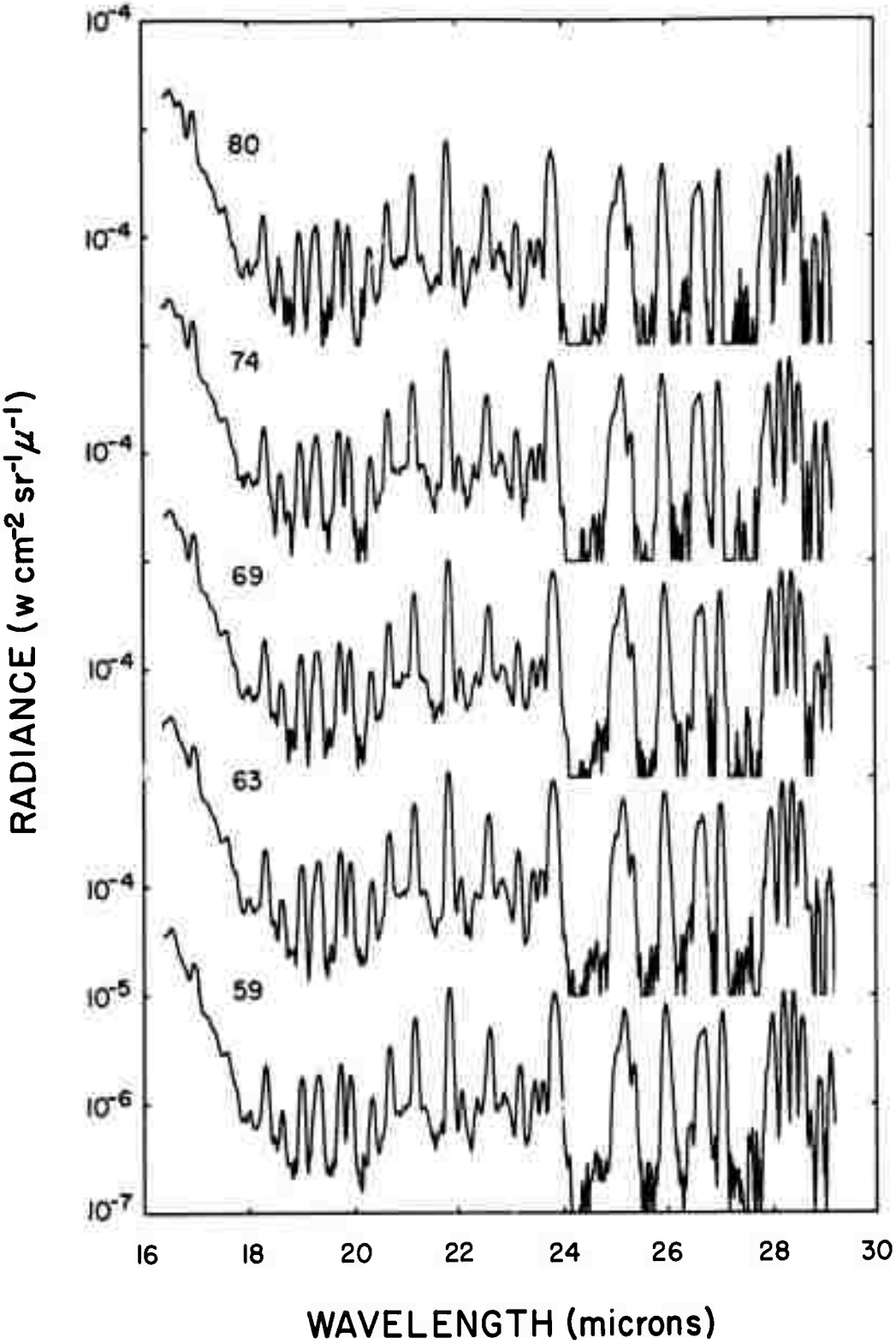
RADIANCE (w cm^{-2} sr$^{-1}\mu^{-1}$)
10^{-4}
10^{-4}
10^{-4}
10^{-4}
10^{-4}
10^{-5}
10^{-6}
10^{-7}
80
74
69
63
59
16
18
20
22
24
26
28
30
WAVELENGTH (microns)

Fig. 1 (b)

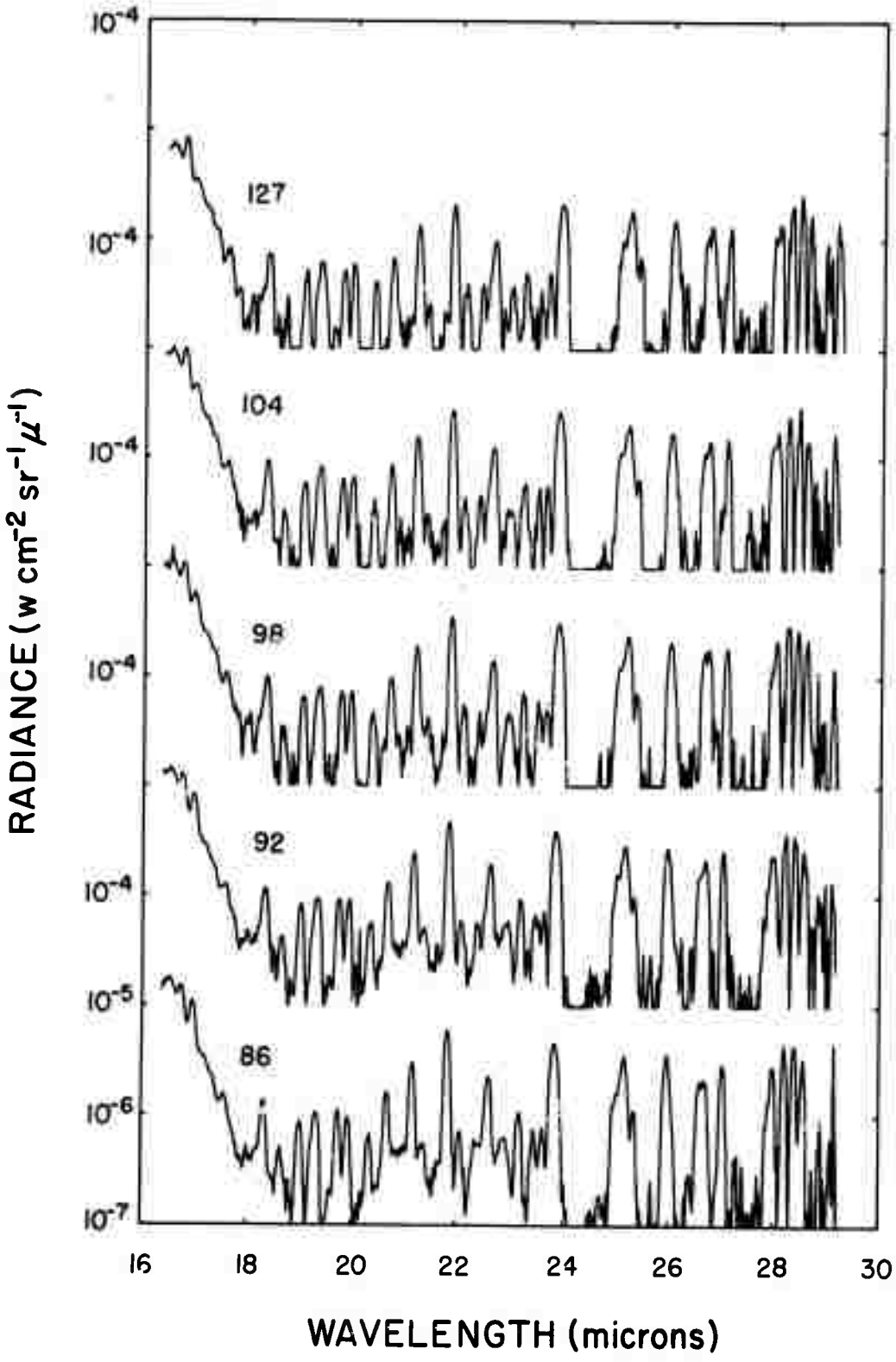
RADIANCE (w cm⁻² sr⁻¹ μ⁻¹)
10⁻⁴
10⁻⁴
10⁻⁴
10⁻⁴
10⁻⁴
10⁻⁵
10⁻⁶
10⁻⁷
127
104
98
92
86
16
18
20
22
24
26
28
30
WAVELENGTH (microns)

Fig. 1 (c)

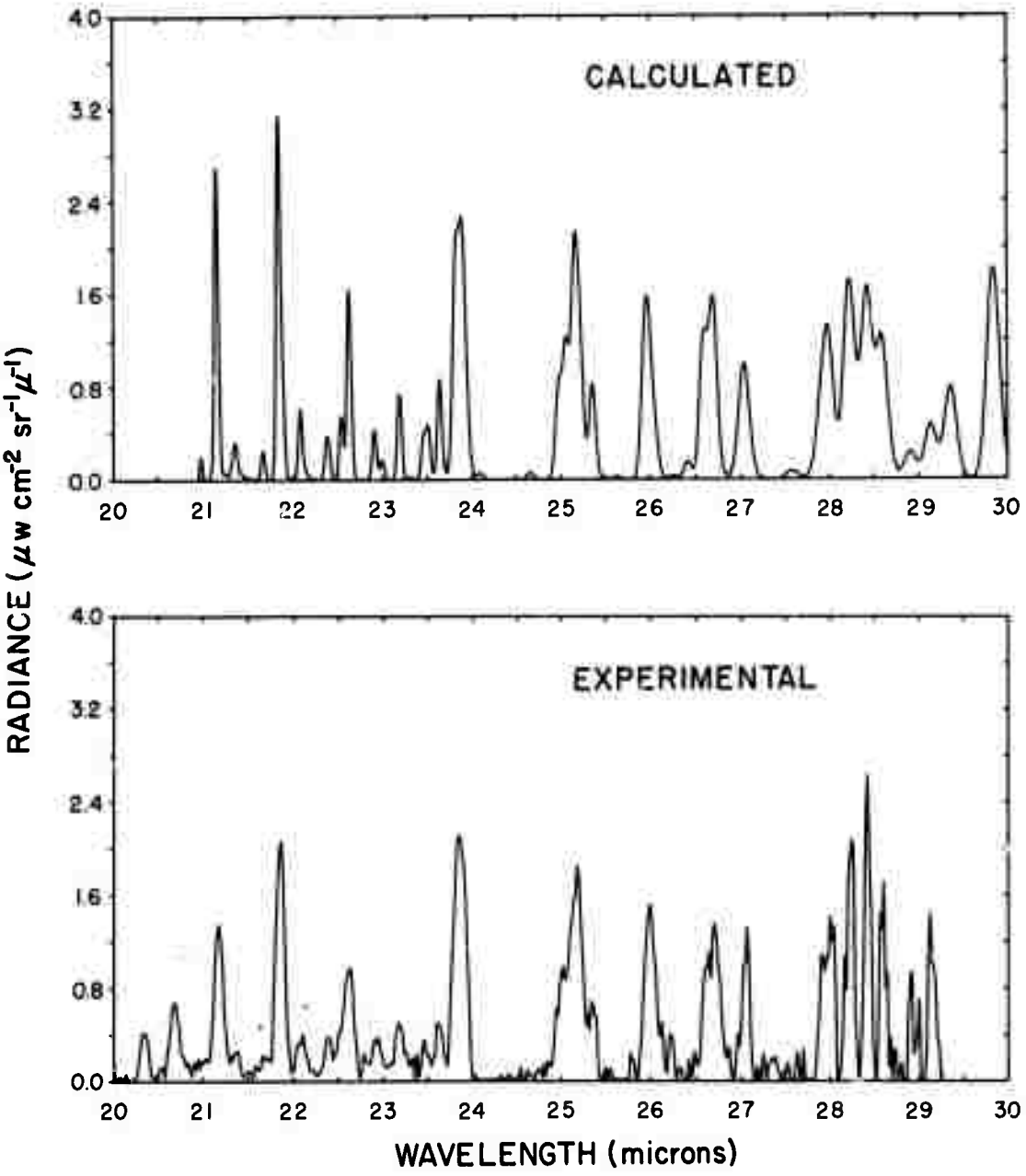
CALCULATED
EXPERIMENTAL
RADIANCE (μw cm⁻² sr⁻¹ μ⁻¹)
WAVELENGTH (microns)
4.0
3.2
2.4
1.6
0.8
0.0
20
21
22
23
24
25
26
27
28
29
30

Fig. 2

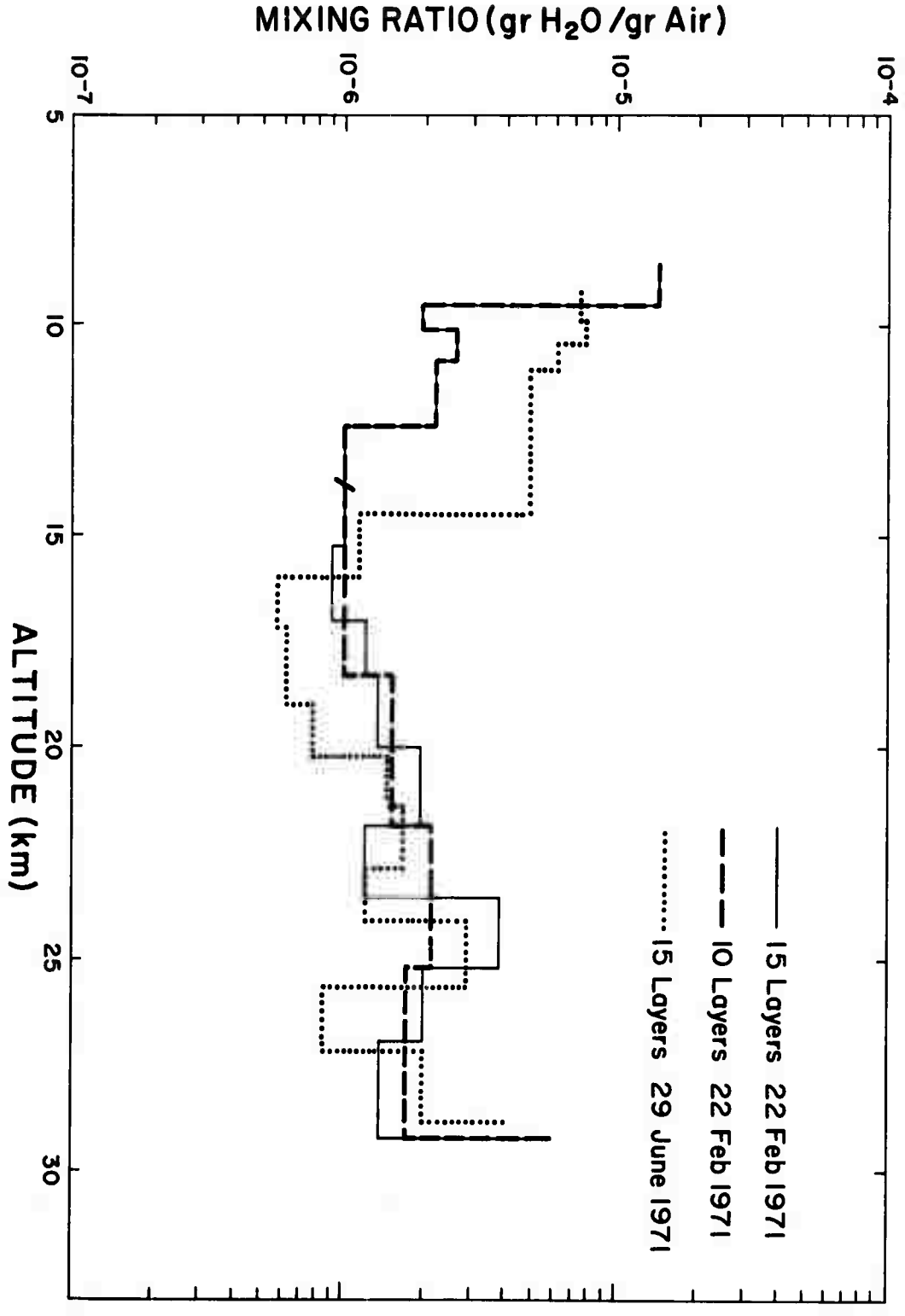
MIXING RATIO (gr H_2O /gr Air)
10^{-7}
10^{-6}
10^{-5}
10^{-4}
ALTITUDE (km)
5
10
15
20
25
30
15 Layers 22 Feb 1971
10 Layers 22 Feb 1971
15 Layers 29 June 1971

Fig. 3

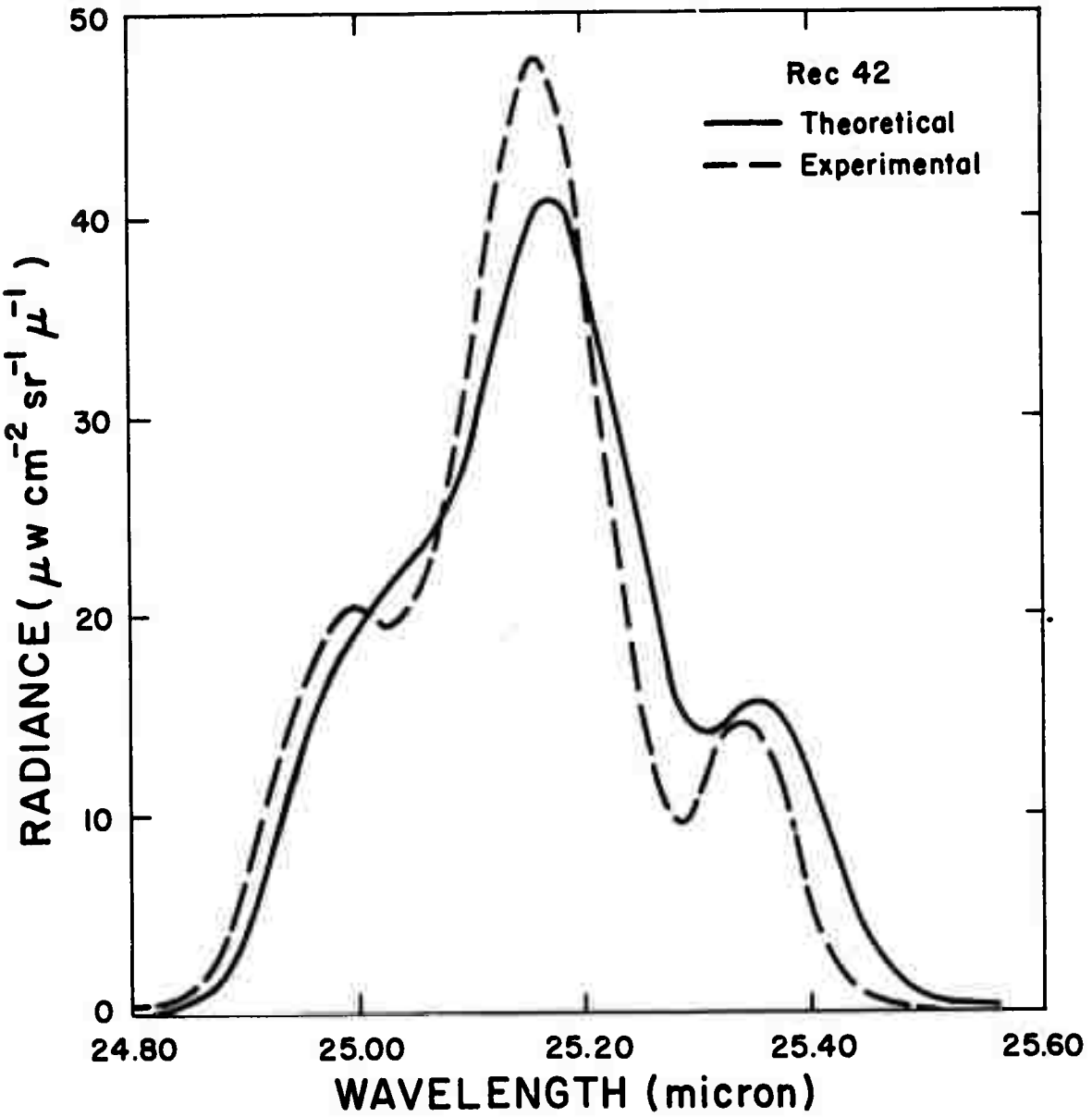
Rec 42
Theoretical
Experimental
RADIANCE (μw cm⁻² sr⁻¹ μ⁻¹)
50
40
30
20
10
0
24.80
25.00
25.20
25.40
25.60
WAVELENGTH (micron)

Fig. 4

Table I

Balloon flight 22 February 1971. Times, Altitudes, Pressures and Temperatures for selected records. The integrated radiance is for the 25μm line group.

Rec	Time MST	Altitude (km)	Pressure (mb)	Temperature (K)	Integrated Radiance ($\mu w cm^{-2} sr^{-1}$)
42	0444	8.6	333.5	237.1	11.89
45	0450	9.5	289.0	229.5	5.03
47	0454	10.2	263.0	224.0	4.36
49	0458	10.9	232.4	217.6	3.49
54	0508	12.5	180.0	216.5	2.36
59	0517	13.9	141.0	216.5	1.96
63	0525	15.2	116.6	216.5	1.71
69	0537	17.0	88.5	216.5	1.47
74	0546	18.3	71.9	216.5	1.30
80	0558	20.1	54.8	216.5	1.12
86	0609	21.8	41.6	218.3	0.93
92	0621	23.6	31.6	220.0	0.84
98	0632	25.2	24.8	221.6	0.66
104	0644	26.9	18.9	223.3	0.57
127	0728	29.3	13.4	225.6	0.52

Table II

Balloon flight 29 June 1971. Times, Altitudes, Pressures and Temperatures for selected records. The integrated radiance is for the 25μm line group.

Rec	Time MST	Altitude (km)	Pressure (mb)	Temperature (K)	Integrated Radiance ($\mu w cm^{-2} sr^{-1}$)
28	0228	9.3	316.0	241.2	11.14
29	0230	9.8	291.7	237.0	9.12
30	0232	10.4	269.4	232.7	7.19
31	0234	11.0	247.6	228.3	5.60
37	0246	14.4	143.5	205.8	1.46
40	0252	15.9	113.2	204.7	1.22
43	0257	17.1	92.0	205.6	1.15
48	0307	18.9	68.3	208.9	1.06
51	0313	20.1	56.3	211.3	1.00
54	0319	21.3	46.7	214.9	0.91
58	0326	22.8	37.1	218.4	0.79
61	0332	24.0	30.8	220.2	0.73
65	0340	25.6	24.2	222.6	0.59
69	0348	27.1	19.2	224.9	0.55
74	0357	28.8	14.8	227.5	0.48